ACS APPLIED MATERIALS & INTERFACES

www.acsami.org

Research Article

# Tuning Electrical and Mechanical Properties of Metal–Organic Frameworks by Metal Substitution

Yabin Yan, Chunyu Wang, Zhengqing Cai, Xiaoyuan Wang,* and Fuzhen Xuan*

Cite This: *ACS Appl. Mater. Interfaces* 2023, 15, 42845–42853

Read Online

ACCESS | Metrics & More | Article Recommendations | Supporting Information



**ABSTRACT:** Metal–organic frameworks (MOFs), synthesized by the self-assembly of organic ligands and metal centers, are structurally designable materials. In the current study, first-principles calculation based on density functional theory (DFT) was performed to investigate the intrinsic mechanical and electrical properties and mechanical–electrical coupling behavior of MOF-5. To improve the conductivity of MOF-5, homologous elements of Cu, Ag, and Au were adopted to replace the Zn atom in MOF-5, reducing the band gap and improving its electrical performance. Cu-MOF-5 and Au-MOF-5, with stable structures, exhibit better conductivity. The intrinsic mechanical properties such as independent elastic constants of MOF-5 and M-MOF-5 (M = Cu, Ag, Au) were obtained. MOF-5 and Cu-MOF-5 were experimentally synthesized to demonstrate the reduction in the band gap after metal substitution. The study of the strain effect of MOF-5 and Cu-MOF-5 proves that strain engineering is an effective method to regulate the band gap and this modulation is repeatable. This study clarifies the tunability of the band gap of MOF-5 with metal substituents and provides an efficient strategy for the development of new types of MOFs with desired physical properties using the combination of theoretical prediction and experimental synthesis and validation.

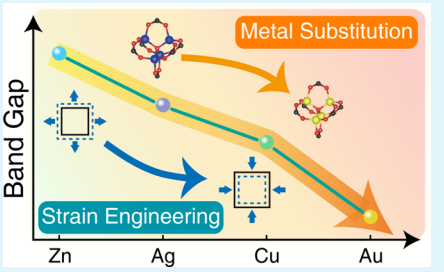


**KEYWORDS:** *metal–organic frameworks, metal substitution, electrical property, mechanical property, strain engineering, first-principles calculation*

## 1. INTRODUCTION

Recently, there has been a rapid development of wearable and portable electronics.[1] Materials that combine high conductivity, structure flexibility, and outstanding strain engineering are crucial for flexible electronics. Metal–organic frameworks (MOFs), which have well-ordered crystalline structures, are constructed from inorganic metal centers and diverse organic linkers through a self-assembly procedure.[2] The flexible framework structures and various combination forms provide the possibility to modify the features of MOFs through the appropriate choice of constituent metal and bridging organic. Due to their excellent porosity and surface area (access to 7140 $m^2/g^3$), early studies in MOFs were primarily focused on separation,[3,4] gas storage,[5] clinical services,[6] and catalysis.[7] MOFs also have potential in photocatalysis,[8] electrocatalysis,[9] chemiresistive sensing,[10] and energy storage technologies.[11] In these applications, identifying MOFs with superior electrical conductivity and flexible structure has attracted considerable attention.

There have been several review articles on the research progress of MOF-related materials for conductivity. Li et al.[12] provided an overview of MOF-based electronic and protic conductors and reported charge transport modes in conductive MOFs. One of the conduction mechanisms is band theory. The band transport mechanism is based on charge carrier delocalization via the conduction or valence band. The engineering of band gaps has been considered significantly in developing practical semiconductors.[13] Wang et al.[14] reported that the clear majority of MOFs are insulators and exhibit very low electronic/ionic conductivity, which is due to the fact that MOFs are usually constructed from O-donor redox-inactive ligands and metal ions, which cannot provide efficient routes for charge transport. Due to the variety of MOF topologies, electronic structure software packages only offer two main modeling approaches.[15] Some consider materials as extended, periodic solids, whereas others treat materials as discrete molecules. In both of them, the electronic structure is the focus of the study. Therefore, various methods such as modifying metal and organic components have been developed to improve the conductivity of MOFs. However, the critical mechanical properties and the mechanical–electrical coupling properties, which are of great importance for the practical application of electronic devices, have been neglected in previous work.

Received: June 12, 2023
Accepted: August 14, 2023
Published: August 29, 2023

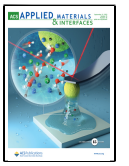

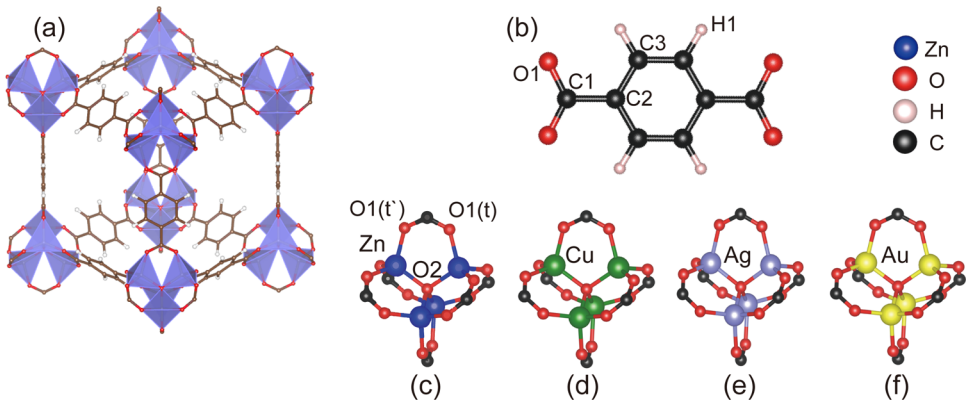


**Figure 1.** Crystal structure of MOF-5. (a) Single cube fragment of MOF-5. (b) Organic linker of benzene-1,4-dicarboxylate (BDC). (c) Structure of the metal-substituted connector of MOF-5. (d) Cu-MOF-5. (e) Ag-MOF-5. (f) Au-MOF-5.

MOF-5 (IRMOF-1), which forms a cubic network from benzene-1,4-dicarboxylate (BDC) and tetrahedral $ZnO_4$ units, is one of the most stable examples of porous 3D-MOFs.[16] As a representative MOF material, MOF-5 exhibits designability and flexible tenability processes of desirable mechanical and thermal stability.[17] However, the low electrical conductivity of MOF-5 significantly restricts its further application in semiconductors. Generally, an insulator is defined by a large band gap ($E_g$), usually over ~4 eV. The band gap of MOF-5 was experimentally determined to be 3.12−3.94 eV,[18−20] indicating the wide-band-gap semiconductor character. The charge-separation state with electrons and holes and a designable structure makes MOF-5 suitable candidates for potential flexible electronics applications. If the band gap of MOF-5 can be tuned to a significantly smaller value, it seems feasible that MOFs could be used in electronic areas. An example of such broadened applications is a gas sensor using semiconducting single-walled carbon nanotubes (SWNTs) with a narrow band gap (~0.5 eV).[21]

From the conductive mechanism, charge mobility can be improved by metal substitution. Spatial and energetic overlap between orbitals plays a dominant role in the charge transport of MOFs. Metal ions with high-energy electrons or holes, which coordinate with organic ligands, are anticipated to form long-range ordered crystal structures, which can enhance orbital overlap between metal ions and organic ligands.[22] Replacing the linker has already been well-studied by Degaga et al.[23] They modified the electronic properties through such ligand functionalization design. In another work, Cedeno et al.[24] combined favorable organic linkers with different functional groups and the band gap of MOFs, which can be fine-tuned. The electronic structures of M-IRMOF (M = Be, Mg, Ca, Zn, and Cd) were investigated by Fuentes-Cabrera et al.;[25] the band gaps are similar to MOF-5 3.5 eV, showing that the conductivity is not improved. Choi et al.[26] considered that the substituted cobalt ions in MOF-5 lead to a narrow band gap. Panda et al.[20] experimentally synthesized MOF-5 and its doped variants (M-MOF-5, M = Co, Ni, Fe, and Mn), and the band gap was found to decrease to 2.63 eV (Fe-MOF-5). A combination of theoretical prediction by density functional theory (DFT) calculation and experimental synthesis and validation provided the opportunity to study and characterize MOF materials based on atomistic-level information and are used as an accelerated investigation and prediction tool.

MOF-5 was found to be a soft and ductile material; when it is deformed by external strain, the electrons redistribute between organic ligands and metals. Wang et al.[27] reported that the external strain will rise the total energy of the system. To maintain the stability of the system, electrons will relax and redistribute, making the electronic activity significantly increase, which improves the conductivity of the material. Previous studies suggested that MOF-5 has Young's modulus over 20 GPa,[28] which is comparable to that of oak wood. At the same time, intrinsic MOF-5 exhibits desirable stability and the linkage breaks until its length changes by more than 20%,[29] which are key factors in modulating its electrical and mechanical properties. Identifying MOFs with high flexibility, conductivity, and sensitivity to strain will provide theoretical support for the electrical and mechanical design of flexible electronics.

Herein, we have employed theoretical calculations to deeply understand the electrical and mechanical properties and mechanical−electrical coupling effect of MOF-5 and M-MOF-5 (M = Cu, Ag, Au) by substituting Zn with homologous elements Cu, Ag, and Au, which are close in size to the atomic radii of Zn atoms. M-MOF-5 (M = Cu, Ag, Au) has been synthesized experimentally and has unique properties in the field of catalysts[30] and antibacterial materials.[31] In general, the DFT methods used here perform well in predicting the elastic and electrical properties of solids and molecules. The basic electrical properties such as the band structure and band gap of MOF-5 and M-MOF (M = Cu, Ag, Au) materials are studied from the perspective of atoms and electrons. The elastic constants and other intrinsic mechanical parameters of MOF-5 and M-MOF (M = Cu, Ag, Au) were obtained by applying different types of strains. MOF-5 and Cu-MOF-5 were experimentally synthesized and characterized by X-ray photoelectron spectroscopy (XPS), scanning electron microscopy (SEM), X-ray crystallography (XRD), and UV−vis to demonstrate a reduction in the band gap. Subsequently, we investigated the mechanical−electrical coupling properties of MOF-5 to modulate the electrical properties by strain engineering.

## 2. COMPUTATIONAL AND EXPERIMENTAL DETAILS

**2.1. Calculation Details.** MOF-5 possesses a highly symmetric three-dimensional framework with the space group of *Fm-3m*. The crystal structure of MOF-5 is shown in Figure 1a. The organic connector and the metal linker are two distinct structural units, as shown in Figure 1b,c, respectively. The crystal structure of MOF-5 contains seven chemically inequivalent atoms (H1, C1, C2, C3, O1, O2, and Zn). In addition, by replacing Zn with Cu, Ag, and Au in the


https://doi.org/10.1021/acsami.3c08470
ACS Appl. Mater. Interfaces 2023, 15, 42845−42853

metal nodes, the metal-substituted connectors of M-MOF-5 are obtained, as illustrated in Figure 1d–f. The structures of M-MOF-5 (M = Cu, Ag, Au) have the same topology as the prototypical MOF-5 with oxide-centered tetrahedra nodes linked by organic molecules (benzene-1,4-dicarboxylate, BDC).

We performed the calculations using the Vienna Ab initio Simulation Package (VASP),[32] which is based on the density functional theory (DFT) method. The generalized gradient approximation (GGA)[33] using Perdew–Wang 91[34] was adopted to describe the exchange–correlation function. The projector-augmented wave method was employed with a cutoff energy of 800 eV. The conjugate gradient method was used for geometry optimizations. For the evaluation of mechanical properties, the Brillouin zone was sampled with the $2 \times 2 \times 2$ $k$-point mesh using the Monkhorst–Pack method. The uniaxial tensile strain was applied to evaluate the mechanical properties of the MOFs. As for the calculation of the electronic band structure of MOFs, we used a denser $k$-point mesh size of $6 \times 6 \times 6$ and the $k$-point path was sampled 20 points in each line.[35] The set of strain engineering is the same as that of electrical properties.

**2.2. Preparation of MOF-5 and Cu-MOF-5.** Zinc nitrate hexahydrate (1.6659 g) and benzene-1,4-dicarboxylate (0.4652 g) were dissolved in 70 mL of dimethylformamide (DMF). After stirring for 1 h at room temperature, the precipitate was transferred to a 140 mL PTFE-lined reactor and reacted at 135 °C for 24 h. The precipitate was washed three times with DMF and ethanol and dried at 80 °C to get MOF-5 in white powder form.

Cu-MOF-5 samples were prepared in a similar procedure to that used for MOF-5. 1.3530 g of copper nitrate trihydrate and 0.4652 g of benzene-1,4-dicarboxylate were dissolved in 70 mL of DMF. After stirring for 1 h at room temperature, the precipitate was transferred to a 140 mL PTFE-lined reactor and reacted at 135 °C for 24 h. The precipitate was washed three times with DMF and ethanol and dried at 80 °C to get Cu-MOF-5 in a blue powder form.

## 3. RESULTS AND DISCUSSION

**3.1. Structural Stability of M-MOF-5.** To examine the thermodynamic stabilities of metal-substituted M-MOF-5, we calculated the cohesive energy by following eq 1

$$E_{coh} = E_{MOF} - (N_{Zn}E_{Zn} + N_C E_C + N_H E_H + N_O E_O)/\sum N_i \quad (1)$$

where $E_i$ and $N_i$ represent the free energy of element $i$ (Zn, C, H, O) and the number of atoms in M-MOF-5, respectively, $E_{coh}$ represents the cohesive energy of M-MOF-5, and $E_{MOF}$ is the free energy of M-MOF-5 in the steady state.

The calculated cohesive energy of MOF-5 and M-MOF-5 is listed in Table 1. The cohesive energy of metal-substituted M-MOF-5 (M = Cu, Ag, Au) is close to that of MOF-5, which indicates that M-MOF-5 retains the same stability as intrinsic MOF-5. In addition, Cu-MOF-5 possesses the lowest cohesive energy of −6.84 eV/atom, indicating the highest structural stability among metal-substituted M-MOF-5.

**Table 1. Cohesive Energy of MOF-5 and M-MOF-5 (M = Cu, Ag, Au)**

| | MOF-5 | Cu-MOF-5 | Ag-MOF-5 | Au-MOF-5 |
|---|---|---|---|---|
| $E_{coh}$ (eV/atom) | −6.83 | −6.84 | −6.68 | −6.64 |

Bond lengths, along with the lattice constants of energy-minimized structures in these systems, are summarized in Table 2. The minimum energy corresponding to the lattice parameters of MOF-5 is 26.076 Å, which is in agreement with the experimental value of $a$ = 25.91 Å.[36] It is convenient to consider each one of M-MOF-5 as made up of connectors and linkers. As it is clear, the variations in the bond lengths of linkers in different structures are negligible, and the maximum difference is 0.6% for C1–C2 in Ag-MOF-5, pointing out that atomic substitution does not affect the structure of the organic linkers. On the other hand, there are significant differences among the connectors of different compounds. The tetrahedral arrangement becomes slightly distorted upon subsisting with the different metals at the Zn site, leading to an increase in the M–O distances. After the replacement of Au and Ag, the M–O1 bond becomes longer, while the bond angle becomes smaller. The maximum differences are 12 and 13% for M–O1 in Ag-MOF-5 and Au-MOF-5, respectively. The same phenomenon was also found when the metal atoms of MOF-5 were replaced by Co, Fe, Ni, Mn, Cd, Be, Mg, and Ca.[20,25] In conclusion, after replacing Zn ions with metal having similar ionic radii, metal substitution only affects the structure of oxide-centered tetrahedra nodes and has almost no effect on the atomic structure of the organic molecules.

**3.2. Electronic Properties of M-MOF-5.** The band structure, total electronic density of states (TDOS), and partial density of states (PDOS) at the equilibrium volumes of MOF-5 are displayed in Figure 2. The band gap between the

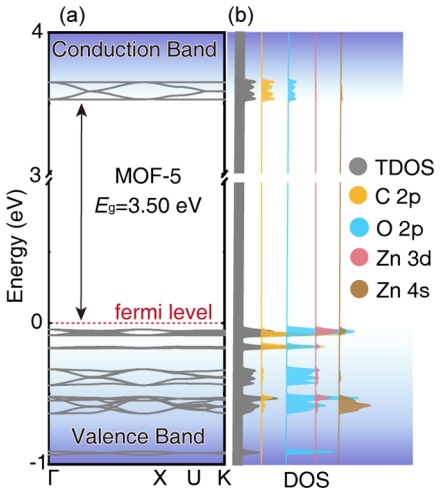


**Figure 2.** (a) Band structure and (b) total density of states (TDOS) and partial density of states (PDOS) of MOF-5. The Fermi level is set to 0 eV.

**Table 2. Structural Parameters of MOF-5 and M-MOF-5 (M = Cu, Ag, Au)**

| | linkers′ structural | | | connectors′ structural | | | |
|---|---|---|---|---|---|---|---|
| material | C1–O1 (Å) | C1–C2 (Å) | C2–C3 (Å) | C3–C3 (Å) | M–O1 | O1–M–O2 (deg) | $a_0$ (Å) |
| MOF-5 | 1.276 | 1.496 | 1.402 | 2.423 | 1.966 | 111.498 | 26.076 |
| Cu-MOF-5 | 1.273 | 1.496 | 1.402 | 2.428 | 1.968 | 112.635 | 25.999 |
| Ag-MOF-5 | 1.272 | 1.505 | 1.401 | 2.426 | 2.207 | 109.518 | 27.319 |
| Au-MOF-5 | 1.273 | 1.503 | 1.401 | 2.424 | 2.229 | 109.587 | 27.379 |


https://doi.org/10.1021/acsami.3c08470
ACS Appl. Mater. Interfaces 2023, 15, 42845–42853

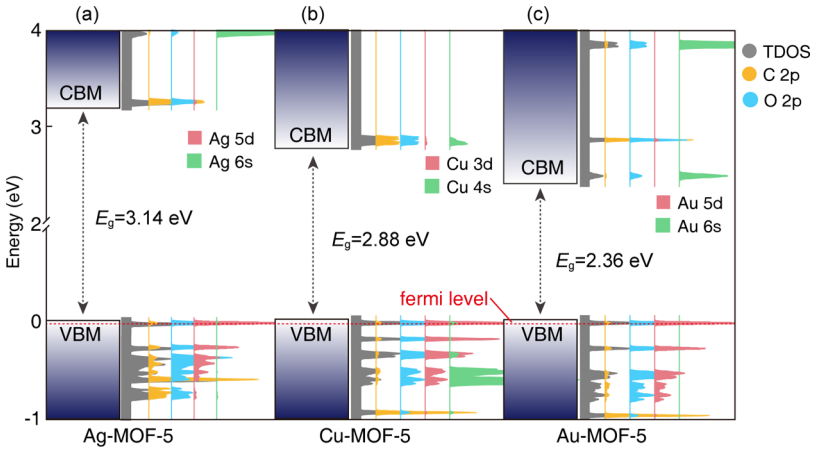


**Figure 3.** Total density of states (TDOS) and partial density of states (PDOS) of (a) Ag-MOF-5, (b) Cu-MOF-5, and (c) Au-MOF-5. The Fermi level is set to 0 eV.

valence band and conduction band is 3.50 eV, which is well consistent with the experimental studies,[19] verifying the wide-band-gap semiconductor character. The distribution of various electronic states in the valence band and the conduction band can be characterized by the PDOS of MOF-5. The p-states of C and O, which dominantly contribute to the valance band and conduction band, are distributed energetically in the same range and thus they can effectively overlap and form very strong covalent bonds. The d-state of Zn is well localized in the valence band, and the d-states of Zn overlap slightly with the p-states of O. This is due to the lack of empty d-orbitals of Zn ions. In the conduction band, the conduction band minimum (CBM) is mainly contributed by p-states of C and O in the energy range between 3.5 and 3.7 eV, which determine the size of the band gap.

As shown in Figure 3, the band gap of M-MOF-5 (M = Ag, Cu, Au) is significantly reduced by the metal substitution. The band gap of Ag-MOF-5, Cu-MOF-5, and Au-MOF-5 is 3.14, 2.88, and 2.36 eV, respectively, indicating conventional semiconductor character. To determine the origin of the reduction of the band gap in M-MOF-5, we calculated their partial density of states (PDOS) in comparison to intrinsic MOF-5. As shown in Figure 3, the electronic structures in M-MOF-5 (M = Ag, Cu, Au) are found to be metallic with DOS across the Fermi level. The valence band maximum (VBM) upshift and the conduction band minimum (CBM) of M-MOF-5 are reduced compared to intrinsic MOF-5, which results in an overall reduction of the band gap after metal substitution.

For the valence band, the density of states of M-MOF-5 is similar, which are mainly contributed by the 2p-states of C and O atoms and the d-states of the metal atom, and the VBM of M-MOF-5 shifts about 0.05 eV in the positive direction. The d-states of Ag, Cu, and Au have obvious resonance with the 2p-states of O with a larger overlap area. The 2p-states of C also have resonance with metal atoms and O, while the contribution is less. The effective mass of charge carriers was affected by the *d*-orbit of the metal atom. Compared to a few contributions of d-states in the prototypical MOF-5, M-MOF-5 exhibits a significant enhancement of d-state contribution. Consequently, the coupling behavior between the organic ligand and intermetal p−d-orbit is increased, which reduces the effective mass of charge carriers of metal-substituted M-MOF-5 and effectively improves the charge mobility on the materials to improve electrical conductivity.

For the conduction band, the CBM structure of Ag-MOF-5 and Cu-MOF-5 are the same as intrinsic MOF-5, which are chiefly donated by p-states of C and O. As for Au-MOF-5 (Figure 3c), the s-states of Au is well localized at CBM, and the Au *s* electrons are transferred to the neighboring O atoms, which leads to ionic bonding between Au and O. This is also consistent with the following analysis of electron localization function. Due to the new chemical bonds formed by Au and O atoms, the band gap of Au-MOF-5 significantly decreased to 2.36 eV, which is reduced by 36% compared to intrinsic MOF-5.

Au-MOF-5, with the lowest band gap of 2.36 eV, exhibits the best conductivity among M-MOF-5 (M = Ag, Cu, Au). To further understand bonding interactions between connectors and linkers, we analyzed the electron localization function (ELF). The electron localization function of MOF-5 and Au-MOF-5 are shown in Figure 4. From Figure 4a, a large value of

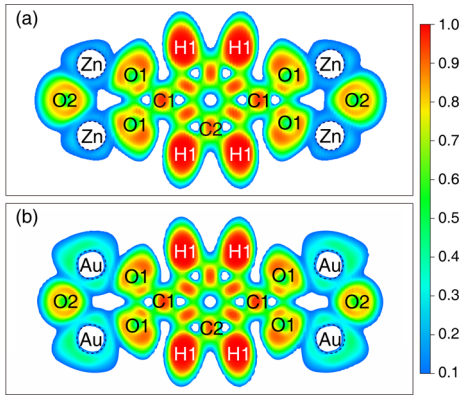


**Figure 4.** Electron localization function (ELF) of (a) MOF-5 and (b) Au-MOF-5.

ELF at the O1 site indicates strongly paired electrons with local bosonic character. The negligibly small ELF between Zn and O atoms and the small value of ELF at the Zn site with spherically symmetric distribution indicates the dominance of the ionic interaction on the bonding interaction between Zn and O sites. The ELF distribution at the O site is not spherically symmetric, and it is polarized toward Zn atoms,


https://doi.org/10.1021/acsami.3c08470
ACS Appl. Mater. Interfaces 2023, 15, 42845−42853

**Table 3. Comparison of Mechanical Properties of MOF-5 and M-MOF-5 (M = Cu, Ag, Au)**

| materials | Young's modulus (GPa) | Poisson's ratio | shear modulus (GPa) | bulk modulus (GPa) | $C_{11}$ (GPa) | $C_{12}$ (GPa) | $C_{44}$ (GPa) |
|---|---|---|---|---|---|---|---|
| MOF-5 | 20.18 | 0.29 | 7.82 | 16.04 | 26.46 | 10.82 | 1.06 |
| Cu-MOF-5 | 10.69 | 0.38 | 3.86 | 15.24 | 20.39 | 12.66 | 1.38 |
| Ag-MOF-5 | 9.40 | 0.36 | 3.45 | 11.46 | 16.06 | 9.16 | 0.73 |
| Au-MOF-5 | 9.54 | 0.40 | 3.42 | 15.24 | 19.79 | 12.96 | 1.38 |

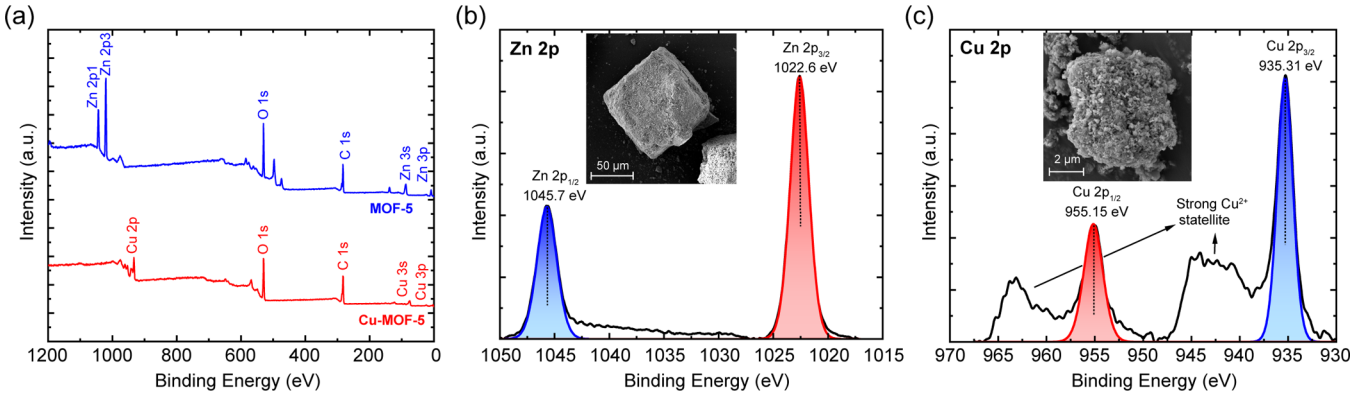


**Figure 5.** (a) XPS spectrum of MOF-5 and Cu-MOF-5, where the chemical components of the sample are labeled. High-resolution XPS and SEM images of (b) MOF-5 and (c) Cu-MOF-5, respectively.

indicating the presence of directional bonding between Zn and O. By comparison, the ELF distribution is relatively large between Au and O (see Figure 4b). It can be inferred that the formation of new chemical bonds between the Au atom and the O atom enhances the electron localization near the metal atom. This corresponds well to Figure 3c above. Formally filled oxygen p orbitals donate electrons into the formally empty s- and d-orbital of the transition metal ions. The Au ion has an empty s-orbital, so there is electron donation from the O p-orbital to the substituent metal *s*-orbital. Therefore, for Au-MOF-5, the interaction between the metal and O orbitals will be enhanced due to the electron donation and the band structure will be changed. This suggests that the metal substitution alters the electronic structure of M-MOF-5, causing a change in the orbital overlap between the ions, which reduces the band gap.

**3.3. Mechanical Properties of M-MOF-5.** The rational design of MOF requires a mechanistic understanding of the framework stability. One possible reason that an evacuated framework becomes unstable at room temperature is elastic instability. To systematically study the intrinsic mechanical properties of MOF-5 and M-MOF-5 (M = Cu, Ag, Au), the elastic constants ($C_{ij}$), Young's modulus, Poisson's ratio, shear modulus, and bulk modulus of materials were calculated, as shown in Table 3.

As MOF-5 belongs to the *Fm-3m* space group, there are three independent elastic constants, $C_{11}$, $C_{12}$, and $C_{44}$, which are listed in in Table 3. The complete set of elastic constants satisfies the condition of cubic crystals imposed by the Born stability criterion,[37] pointing to a mechanically stable M-MOF-5. As MOF-5 is an anisotropic material, the ELAM (Elastic Anisotropy Measures) code[38] is adopted to calculate the anisotropic mechanical properties of MOF-5. Calculation details for each modulus are given in the Supporting Information. The calculated Young's modulus of MOF-5 is 20.18 GPa, which is in agreement with the previous study (21.6 GPa).[28] The bulk and shear moduli can be used to predict the brittle and ductile behavior of materials. As shown in Table 3, after the metal substitution, M-MOF-5 shows better ductility with lower shear moduli (~3 GPa) compared to intrinsic MOF-5 7.82 GPa. It should be noted that the materials calculated by the DFT method are perfect, without defects, so we have used the shear moduli obtained under tiny strains to quantify ductility instead of the fracture strain.

As Table 3 shown, MOF-5 and metal-substituted MOFs are soft, ductile, and compressible materials. Young's modulus, shear modulus, and bulk modulus of M-MOF-5 decrease after atomic replacement, and the mechanical properties of Cu-MOF-5 and Au-MOF-5 change relatively obviously, and the ability of materials to resist deformation becomes weak. Young's modulus of modified MOFs is half (~10 GPa) of that of the prototypical MOF-5 (~20 GPa), indicating that new MOFs are more suitable for flexible sensors than classic MOF-5.

The bulk modulus of intrinsic MOF-5 is 16.04 GPa, which is reduced by 28.6% after metal substituent as Ag-MOF-5. The calculated bulk modulus indicates that M-MOF-5 (M = Cu, Ag, Au) is an easily compressible system. Its compressibility is mostly determined by the presence of the BDC linkers, which offer almost the same kind of resistance to an external strain as found for graphite. The elastic properties of such a metal−organic system can be understood by its structural topology. M-MOF-5 is made of highly porous organic frameworks held together by strong metal−oxygen−carbon bonds. The linkage between metal oxides and the organic ligands generates a rather soft material with relatively small elastic moduli.

$C_{44}$ indicates the stability of the material.[39] Shear strain is the most vulnerable deformation for MOF-5 with small-shear-modulus $C_{44}$. The calculated results of Table 3 confirmed a small $C_{44}$ of MOF-5 (1.06 GPa). Smaller $C_{44}$ also indicates that MOF-5 can be disintegrated into potentially useful structures under certain shear stress. For example, the prototypical MOF-5 structure has a large pore volume, but the pores are too open to maintain hydrogen molecules at high temperatures and collapsed M-MOF-5 with smaller cavities connected through smaller channels, which, in principle, favors $H_2$ storage.


https://doi.org/10.1021/acsami.3c08470
ACS Appl. Mater. Interfaces 2023, 15, 42845−42853

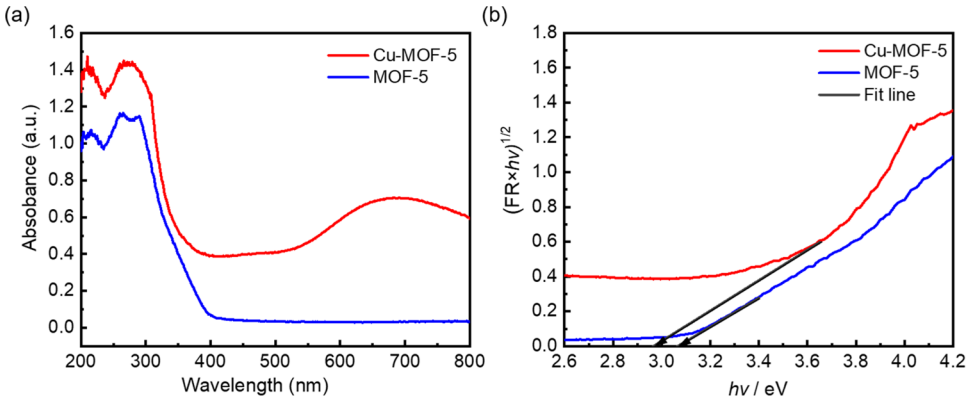


**Figure 6.** (a) UV−vis diffused reflectance spectra and (b) the Tauc plot of MOF-5 and Cu-MOF-5. The linear part of the plot is extrapolated to the *x*-axis.

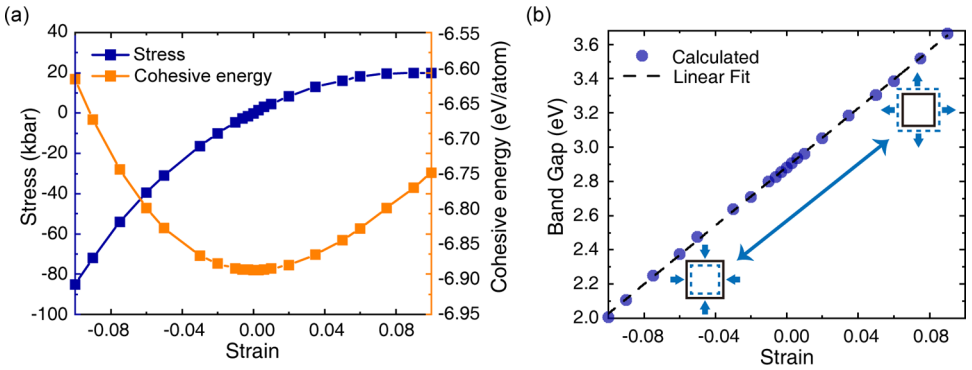


**Figure 7.** Variation of the (a) cohesive energy and stress and (b) band gap of Cu-MOF-5 with the applied mechanical strain.

Moreover, we verify that MOF-5 and Ag-MOF are close to being structurally unstable. Nevertheless, Cu-MOF and Au-MOF with higher values of $C_{44}$ (1.38 GPa) possess better structural stability. It is expected that a combination of high conductivity and flexible structure with enhanced stability could be obtained through metal substitution.

**3.4. UV−vis Spectra of M-MOF-5.** With the help of theoretical calculations, we have screened out materials with excellent electrical and mechanical properties after the substitution of metal atoms. Cu-MOF-5 with higher $C_{44}$ (∼1.4 GPa) and lower cohesive energy (∼ −6.8 eV/atom) are more stable and flexible than the prototypical MOF-5. To investigate the effect of metal substitution on the electrical properties, we experimentally prepared MOF-5 and Cu-MOF-5 for comparison. The XPS spectrum (Figure 5a) suggests that Zn atoms were substituted by Cu completely. Figure 5b,c shows the scanning electron microscopy (SEM) images of MOF-5 and Cu-MOF-5, which are cubic in shape with a rough surface. High-resolution XPS (Figure 5b,c) was also employed to investigate the composition and the chemical bonds of the samples. The Zn 2p spectrum (Figure 5b) showed that two fitted peaks were located at the bonding energies of 1045.7 and 1022.6 eV, corresponding to Zn $2p_{1/2}$ and Zn $2p_{3/2}$, respectively. The Cu 2p spectrum (Figure 5c) clearly shows two different peaks, which are located at the bonding energies of 955.15 and 935.31 eV, corresponding to Cu $2p_{1/2}$ and Cu $2p_{3/2}$, respectively. As expected, the Cu atom completely replaces the Zn atom and forms Cu-MOF-5. This further demonstrates that the method reported in this work is effective in the preparation of M-MOF-5. X-ray diffraction (XRD) results can be found in Figure S1 in the Supporting Information, which show more details about the crystal structures of intrinsic MOF-5 and Cu-MOF.

UV−vis is the spectra used to analyze the optical absorption and optical band gap ($E_g$) of the synthesized samples. It can be seen from Figure 6a that both MOF-5 and Cu-MOF-5 have better absorption in the ultraviolet range. Intrinsic MOF-5 shows strong absorption in the UV region with a wavelength $\lambda$ of 264 and 291 nm, which is well consistent with previous studies.[20,40] After the metal substitution, Cu-MOF-5 exhibits two absorption peaks at $\lambda$ of 210 and 267 nm.

The computational calculations predict a downward shift of the conduction band position due to the form of new chemical bonds, which nicely corresponds to the data in Figure 6b. The band gap of the synthesized samples was estimated using the Tauc method,[41] and the band gap ($E_g$) can be obtained by the formula $E_g$ (eV) = 1240/$\lambda$ (nm). As a result of the metal substitution, the band gap is reduced from 3.10 eV (MOF-5) to 2.97 eV (Cu-MOF-5), which confirms our DFT calculation results and previous experiment reports.[18] This synthesis confirms that Cu can occupy the Zn position in the MOF-5 topology, providing the routes for the rational design of MOFs with the targeted electronic structure.

**3.5. Strain Engineering of Electrical Properties of M-MOF-5.** The variation trend of Cu-MOF-5 cohesion energy and stress with external hydrostatic strain is depicted in Figure 7a. The material's stability decreases as the strain increases continuously. Tensile-compression asymmetry exists in the change of cohesion energy and stress. It is worth noting that even when the material is severely deformed to a hydrostatic strain of −0.1, the structure retains a low cohesive energy (−6.60 eV/atom), pointing out that Cu-MOF-5 has a high


https://doi.org/10.1021/acsami.3c08470
ACS Appl. Mater. Interfaces 2023, 15, 42845−42853

resistance to deformation. The compressive strain is achievable in practice with cutting-edge in situ transmission and scanning electron microscopy techniques.[42] Figure 7b shows the variation of the band gap of Cu-MOF-5 with the mechanical strain. The strain is applied in three directions. The band gap decreases linearly with the increment of the compression strain ($\varepsilon_c$). When $\varepsilon_c = -0.1$, the band gap of Cu-MOF-5 decreases to 2.00 eV, indicating a semiconductor character. However, with a tension strain ($\varepsilon_T$), the impedance shows a linear increment, and the band gap reaches a value of 3.66 eV at $\varepsilon_T = 0.1$, which indicates a significant transition of Cu-MOF-5 to a wide-band-gap semiconductor. Thus, strain engineering is an effective method to tune the electrical properties of MOFs.

The band gap of Cu-MOF-5 is reduced by 20% (2.00 eV) compared to intrinsic MOF-5 (2.76 eV[27]) at the same compressive strain of 0.1. Therefore, the electrical properties of Cu-MOF-5 are more sensitive to strain engineering. In addition, the band gap of intrinsic MOF-5 decreased with the increment of both tension and compression strain.[27] In contrast, the band gap of Cu-MOF-5 varies linearly with the applied strain. A small band gap can be obtained when compressed and a wide band gap when stretched, which means the electrical properties of MOF can be repeatedly modulated with external strain. In the current study, we have confirmed that Cu-MOF-5 can be stable within the strain range of −0.1−0.1. With the applied strain, the volume of Cu-MOF-5 changes accordingly. As illustrated in Figure 7b, the band gap of Cu-MOF-5 is positively correlated with the volume change, indicating that Cu-MOF-5 exhibits negative deformation potential,[43] thus showing a linear relationship between the band gap of Cu-MOF-5 and the applied strain.

## 4. CONCLUSIONS

In summary, the electronic and mechanical properties and the mechanical−electrical coupling behavior of intrinsic MOF-5 and M-MOF-5 (M = Ag, Cu, Au) are systematically studied by the first-principles calculation and validated by the experiment. MOF-5 is found to be a wide-band-gap semiconductor material with a band gap of 3.5 eV. The band gap is greatly reduced by replacing Zn with Cu, Au, or Ag ions. Especially for Cu-MOF and Au-MOF, $E_g$ after metal nodes substituent reduced by 33%, are only 2.3−2.8 eV, indicative of excellent semiconductor character. The calculated mechanical properties of M-MOF-5, such as Young's modulus, Poisson's ratio, shear modulus, bulk modulus, and elastic constants ($C_{ij}$), indicate that M-MOF-5 are soft, ductile, and compressible materials. Au-MOF-5 and Cu-MOF-5 with higher $C_{44}$ (∼1.4 GPa) and lower Young's modulus (∼10 GPa) are more stable and flexible than the prototypical MOF-5. We have synthesized the most stable Cu-MOF-5 in M-MOF-5 in the experiments and demonstrated that metal substitution can reduce the band gap. The strain engineering of Cu-MOF-5 shows that strain engineering is an effective method to regulate the band gap, which shows important implications for the development of electronic devices such as sensors. The selected metal substituent M-MOF-5 is worked out in theory and validated by the experiment, which starts from theoretical calculations and ends with material properties characterization, providing a theoretical prediction and experimental validation-based research strategy for the development of new MOFs. This strategy is applicable to a new MOF architecture and can serve as a roadmap for the future synthesis of MOFs with predefined properties.

## ASSOCIATED CONTENT

### Supporting Information

The Supporting Information is available free of charge at https://pubs.acs.org/doi/10.1021/acsami.3c08470.

Characterization of the experiment; details of theory calculations; elements content of experimentally synthesized MOF-5; element content of experimentally synthesized Cu-MOF-5; XRD patterns of Cu-MOF-5 and MOF-5; and variation of cohesive energy and stress with the applied mechanical strain of MOF-5 (PDF)

## AUTHOR INFORMATION


### Corresponding Authors

**Xiaoyuan Wang** − *Shanghai Key Laboratory for Intelligent Sensing and Detection Technology, East China University of Science and Technology, Shanghai 200237, China; Key Laboratory of Pressure Systems and Safety Ministry of Education, School of Mechanical and Power Engineering, East China University of Science and Technology, Shanghai 200237, China*; Email: wangxiaoyuan@ecust.edu.cn

**Fuzhen Xuan** − *Shanghai Key Laboratory for Intelligent Sensing and Detection Technology, East China University of Science and Technology, Shanghai 200237, China; Key Laboratory of Pressure Systems and Safety Ministry of Education, School of Mechanical and Power Engineering, East China University of Science and Technology, Shanghai 200237, China*; Email: fzxuan@ecust.edu.cn

### Authors

**Yabin Yan** − *Shanghai Key Laboratory for Intelligent Sensing and Detection Technology, East China University of Science and Technology, Shanghai 200237, China; Key Laboratory of Pressure Systems and Safety Ministry of Education, School of Mechanical and Power Engineering, East China University of Science and Technology, Shanghai 200237, China*; orcid.org/0000-0002-1014-3860

**Chunyu Wang** − *Shanghai Key Laboratory for Intelligent Sensing and Detection Technology, East China University of Science and Technology, Shanghai 200237, China; Key Laboratory of Pressure Systems and Safety Ministry of Education, School of Mechanical and Power Engineering, East China University of Science and Technology, Shanghai 200237, China*; orcid.org/0000-0002-3093-0220

**Zhengqing Cai** − *National Engineering Research Center of Industrial Wastewater Detoxication and Resource Recovery, East China University of Science and Technology, Shanghai 200237, China*; orcid.org/0000-0001-8253-1558

Complete contact information is available at: https://pubs.acs.org/10.1021/acsami.3c08470


### Author Contributions

This manuscript was written through contributions of all authors.

### Notes

The authors declare no competing financial interest.

## ACKNOWLEDGMENTS

Y.Y. thanks the support of the National Natural Science Foundation of China (Grant No. 52275149) and the Program for Professor of Special Appointment (Eastern Scholar) at Shanghai Institutions of Higher Learning. F.X. thanks the

support of the National Natural Science Foundation of China (Grant No. 51835003).

## REFERENCES

(1) Erçarıkcı, E.; Dağcı Kıranşan, K.; Topçu, E. Three-Dimensional ZnCo-MOF Modified Graphene Sponge: Flexible Electrode Material for Symmetric Supercapacitor. *Energy Fuels* **2022**, *36*, 1735−1745.
(2) Li, H.; Eddaoudi, M.; et al. Design and Synthesis of an Exceptionally Stable and Highly Porous Metal-organic Framework. *Nature* **1999**, *402*, 276−279.
(3) Farha, O. K.; Eryazici, I.; Jeong, N. C.; Hauser, B. G.; Wilmer, C. E.; Sarjeant, A. A.; Snurr, R. Q.; Nguyen, S. T.; Yazaydın, A. Ö.; Hupp, J. T. Metal-Organic Framework Materials with Ultrahigh Surface Areas: Is the Sky the Limit? *J. Am. Chem. Soc.* **2012**, *134*, 15016−15021.
(4) Sun, T.; Hao, S.; Fan, R.; Qin, M.; Chen, W.; Wang, P.; Yang, Y. Hydrophobicity-Adjustable MOF Constructs Superhydrophobic MOF-rGO Aerogel for Efficient Oil−Water Separation. *ACS Appl. Mater. Interfaces* **2020**, *12*, 56435−56444.
(5) Gao, Z.; Liang, L.; Zhang, X.; Xu, P.; Sun, J. Facile One-Pot Synthesis of Zn/Mg-MOF-74 with Unsaturated Coordination Metal Centers for Efficient $CO_2$ Adsorption and Conversion to Cyclic Carbonates. *ACS Appl. Mater. Interfaces* **2021**, *13*, 61334−61345.
(6) Biswas, S.; Lan, Q.; Xie, Y.; Sun, X.; Wang, Y. Label-Free Electrochemical Immunosensor for Ultrasensitive Detection of Carbohydrate Antigen 125 Based on Antibody-Immobilized Biocompatible MOF-808/CNT. *ACS Appl. Mater. Interfaces* **2021**, *13*, 3295−3302.
(7) Tuttle, R. R.; Folkman, S. J.; Rubin, H. N.; Finke, R. G.; Reynolds, M. M. Copper Metal-Organic Framework Surface Catalysis: Catalyst Poisoning, IR Spectroscopic, and Kinetic Evidence Addressing the Nature and Number of the Catalytically Active Sites En Route to Improved Applications. *ACS Appl. Mater. Interfaces* **2020**, *12*, 39043−39055.
(8) Jafarzadeh, M. Recent Progress in the Development of MOF-Based Photocatalysts for the Photoreduction of Cr(VI). *ACS Appl. Mater. Interfaces* **2022**, *14*, 24993−25024.
(9) Ahsan, M. A.; He, T.; Eid, K.; Abdullah, A. M.; Sanad, M. F.; Aldalbahi, A.; Alvarado-Tenorio, B.; Du, A.; Puente Santiago, A. R.; Noveron, J. C. Controlling the Interfacial Charge Polarization of MOF-Derived 0D−2D vdW Architectures as a Unique Strategy for Bifunctional Oxygen Electrocatalysis. *ACS Appl. Mater. Interfaces* **2022**, *14*, 3919−3929.
(10) Meng, Z.; Stolz, R. M.; Mirica, K. A. Two-Dimensional Chemiresistive Covalent Organic Framework with High Intrinsic Conductivity. *J. Am. Chem. Soc.* **2019**, *141*, 11929−11937.
(11) Liu, N.; Chai, L.; Senthil, R. A.; Li, W.; Krishnamoorthy, M.; Sun, Y.; Liu, X.; Qian, J.; Li, X.; Pan, J. Couple of Nonpolarized/Polarized Electrodes Building a New Universal Electrochemical Energy Storage System with an Impressive Energy Density. *ACS Appl. Mater. Interfaces* **2021**, *13*, 45375−45384.
(12) Li, W. H.; Deng, W. H.; Wang, G. E.; Xu, G. Conductive MOFs. *EnergyChem* **2020**, *2*, No. 100029.
(13) Usman, M.; Mendiratta, S.; Lu, K. Semiconductor Metal-Organic Frameworks: Future Low-Bandgap Materials. *Adv. Mater.* **2017**, *29*, No. 1605071.
(14) Wang, H. N.; Meng, X.; Dong, L. Z.; Chen, Y.; Li, S. L.; Lan, Y. Q. Coordination Polymer-Based Conductive Materials: Ionic Conductivity Vs. Electronic Conductivity. *J. Mater. Chem. A* **2019**, *7*, 24059−24091.
(15) Mancuso, J. L.; Mroz, A. M.; Le, K. N.; Hendon, C. H. Electronic Structure Modeling of Metal-Organic Frameworks. *Chem. Rev.* **2020**, *120*, 8641−8715.
(16) Li, H.; Davis, C. E.; Groy, T. L.; Kelley, D. G.; Yaghi, O. M. Coordinatively Unsaturated Metal Centers in the Extended Porous Framework of Zn3(BDC)3·6CH3OH (BDC = 1,4-Benzenedicarboxylate). *J. Am. Chem. Soc.* **1998**, *120*, 2186−2187.
(17) Tranchemontagne, D. J.; Hunt, J. R.; Yaghi, O. M. Room Temperature Synthesis of Metal-Organic Frameworks: MOF-5, MOF-74, MOF-177, MOF-199, and IRMOF-0. *Tetrahedron* **2008**, *64*, 8553−8557.
(18) Thakare, S. R.; Ramteke, S. M. Postmodification of MOF-5 Using Secondary Complex Formation Using 8-Hydroxyquinoline (HOQ) for the Development of Visible Light Active Photocatalysts. *J. Phys. Chem. Solids* **2018**, *116*, 264−272.
(19) Alvaro, M.; Carbonell, E.; Ferrer, B.; Xamena, F. X. L.; Garcia, H. Semiconductor Behavior of a Metal-Organic Framework (MOF). *Chem. - Eur. J.* **2007**, *13*, 5106−5112.
(20) Panda, J.; Singha, D.; Panda, P. K.; Tripathy, B. C.; Rana, M. K. Experimental and DFT Study of Transition Metal Doping in a Zn-BDC MOF to Improve Electrical and Visible Light Absorption Properties. *J. Phys. Chem. C* **2022**, *126*, 12348−12360.
(21) Kong, J.; Franklin, N. R.; Zhou, C.; Chapline, M. G.; Peng, S.; Cho, K.; Dai, H. Nanotube Molecular Wires as Chemical Sensors. *Science* **2000**, *287*, 622−625.
(22) Li, C.; Sunc, X.; Yaode, Y.; Hongab, G. Recent Advances of Electrically Conductive Metal-Organic Frameworks in Electrochemical Applications. *Mater. Today Nano* **2021**, *13*, No. 100105.
(23) Degaga, G. D.; Pandey, R.; Gupta, C.; Bharadwaj, L. Tailoring of the Electronic Property of Zn-BTC Metal-Organic Framework: Via Ligand Functionalization: An Ab Initio Investigation. *RSC Adv.* **2019**, *9*, 14260−14267.
(24) Cedeno, R. M.; Cedeno, R.; Gapol, M. A.; Lerdwiriyanupap, T.; Impeng, S.; Flood, A.; Bureekaew, S. Bandgap Modulation in Zr-Based Metal-Organic Frameworks by Mixed-Linker Approach. *Inorg. Chem.* **2021**, *60*, 8908−8916.
(25) Fuentes-Cabrera, M.; Nicholson, D. M.; Sumpter, B. G.; Widom, M. Electronic Structure and Properties of Isoreticular Metal-Organic Frameworks: The Case of M-IRMOF1 (M=Zn, Cd, Be, Mg, and Ca). *J. Chem. Phys.* **2005**, *123*, No. 124713.
(26) Choi, J. H.; Choi, Y. J.; Lee, J. W.; Shin, W. H.; Kang, J. K. Tunability of Electronic Band Gaps from Semiconducting to Metallic States via Tailoring Zn ions in MOFs with Co ions. *Phys. Chem. Chem. Phys.* **2009**, *11*, 628−631.
(27) Xiao-Yuan, W.; Feng-Peng, Z.; Jie, W.; Ya-Bin, Y. First-Principle Studies of Mechanical, Electronic Properties and Strain Engineering of Metal-Organic Framework. *Acta Phys. Sin.* **2016**, *65*, 178105.
(28) Bahr, D. F.; Reid, J. A.; Mook, W. M.; Bauer, C. A.; Stumpf, R.; Skulan, A. J.; Moody, N. R.; Simmons, B. A.; Shindel, M. M.; Allendorf, M. D. Erratum: Mechanical Properties of Cubic Zinc Carboxylate IRMOF-1 Metal-Organic Framework Crystals [Phys. Rev. B 76, 184106 (2007)]. *Phys. Rev. B* **2008**, *77*, No. 059902.
(29) Zheng, B.; Fu, F.; Wang, L. L.; Wang, J.; Du, L.; Du, H. Effect of Defects on the Mechanical Deformation Mechanisms of Metal-Organic Framework-5: A Molecular Dynamics Investigation. *J. Phys. Chem. C* **2018**, *122*, 4300−4306.
(30) Müller, M.; Hermes, S.; Kähler, K.; van den Berg, M. W. E.; Muhler, M.; Fischer, R. A. Loading of MOF-5 with Cu and ZnO Nanoparticles by Gas-Phase Infiltration with Organometallic Precursors: Properties of Cu/ZnO@MOF-5 as Catalyst for Methanol Synthesis. *Chem. Mater.* **2008**, *20*, 4576−4587.
(31) Hu, Y.; Yang, H.; Wang, R.; Duan, M. Fabricating Ag@MOF-5 Nanoplates by the Template of MOF-5 and Evaluating its Antibacterial Activity. *Colloids Surf., A* **2021**, *626*, No. 127093.
(32) Kresse, G.; Furthmüller, J. Efficiency of Ab-Initio Total Energy Calculations for Metals and Semiconductors Using a Plane-Wave Basis Set. *Comput. Mater. Sci.* **1996**, *6*, 15−50.
(33) Perdew, J. P.; Burke, K.; Wang, Y. Generalized Gradient Approximation for the Exchange-Correlation Hole of a Many-Electron System. *Phys. Rev. B* **1996**, *54*, 16533−16539.
(34) Burke, K.; Perdew, J. P.; Wang, Y. Derivation of a Generalized Gradient Approximation: The PW91 Density Functional. In *Electronic Density Functional Theory*; Springer, 1998, 81−111 DOI: 10.1007/978-1-4899-0316-7_7.
(35) Monkhorst, H. J.; Pack, J. D. Special Points for Brillouin-Zone Integrations. *Phys. Rev. B* **1976**, *13*, 5188.

(36) Yildirim, T.; Hartman, M. Direct Observation of Hydrogen Adsorption Sites and Nanocage Formation in Metal-Organic Frameworks. *Phys. Rev. Lett.* **2005**, *95*, No. 215504.
(37) Mouhat, F.; Coudert, F. X. Necessary and Sufficient Elastic Stability Conditions in Various Crystal Systems. *Phys. Rev. B* **2014**, *90*, No. 224104.
(38) Marmier, A.; Lethbridge, Z. A. D.; Walton, R. I.; Smith, C. W.; Parker, S. C.; Evans, K. E. ElAM: A Computer Program for the Analysis and Representation of Anisotropic Elastic Properties. *Comput. Phys. Commun.* **2010**, *181*, 2102−2115.
(39) Samanta, A.; Furuta, T.; Li, J. Theoretical Assessment of the Elastic Constants and Hydrogen Storage Capacity of Some Metal-Organic Framework Materials. *J. Chem. Phys.* **2006**, *125*, No. 084714.
(40) Hang, Z.; Yu, H.; Luo, L.; Huai, X. Nanoporous g-C3N4/MOF: High-Performance Photoinitiator for UV-Curable Coating. *J. Mater. Sci.* **2019**, *54*, 13959−13972.
(41) Makuła, P.; Pacia, M.; Macyk, W. How to Correctly Determine the Band Gap Energy of Modified Semiconductor Photocatalysts Based on UV−Vis Spectra. *J. Phys. Chem. Lett.* **2018**, *9*, 6814−6817.
(42) Xing, Y.; Luo, L.; Li, Y.; Wang, D.; Hu, D.; Li, T.; Zhang, H. Exploration of Hierarchical Metal-Organic Framework as Ultralight, High-Strength Mechanical Metamaterials. *J. Am. Chem. Soc.* **2022**, *144*, 4393−4402.
(43) Van de Walle, C. G.; Martin, R. M. "Absolute" Deformation Potentials: Formulation and Ab Initio Calculations for Semiconductors. *Phys. Rev. Lett.* **1989**, *62*, 2028.


https://doi.org/10.1021/acsami.3c08470
*ACS Appl. Mater. Interfaces* 2023, 15, 42845−42853